

# $CP$ -violation in the production of $\tau$ -leptons at TESLA with beam polarization

B. Ananthanarayan<sup>1</sup>, S.D. Rindani<sup>2</sup>, A. Stahl<sup>3</sup>

<sup>1</sup> Centre for Theoretical Studies, Indian Institute of Science, Bangalore 560 012, India

<sup>2</sup> Theory Group, Physical Research Laboratory, Navrangpura, Ahmedabad 380 009, India

<sup>3</sup> DESY, Platanenallee 6, 15738 Zeuthen, Germany

Received: 13 June 2002 / Revised version: 17 October 2002

Published online: 20 December 2002 – © Springer-Verlag / Società Italiana di Fisica 2002

**Abstract.** We study the prospects of discovering  $CP$ -violation in the production of  $\tau$  leptons in the reaction  $e^+e^- \rightarrow \tau^+\tau^-$  at TESLA, an  $e^+e^-$  linear collider with center-of-mass energies of 500 or even 800 GeV. Non-vanishing expectation values of certain correlations between the momenta of the decay products of the two  $\tau$  leptons would signal the presence of  $CP$ -violation beyond the standard model. We study how longitudinal beam polarization of the electron and positron beams will enhance these correlations. We find that  $T$ -odd and  $T$ -even vector correlations are well suited for the measurements of the real and imaginary parts of the electric dipole form factors. We expect measurements of the real part with a precision of roughly  $10^{-20}$  e cm and of the imaginary part of  $10^{-17}$  e cm. This compares well with the size of the expected effects in many extensions of the standard model.

## 1 Introduction

One possible signal for physics beyond the standard model (SM) would be the presence of significant  $CP$ -violation in the production of  $\tau$  leptons [1, 2], or in their decay [3].  $CP$ -violation in production would arise, assuming that  $e^+e^-$  annihilate into a virtual  $\gamma$  or  $Z$ , from the electric dipole form factor (EDM)  $d_\tau^\gamma(q^2)$ , or its generalization for the  $Z$  coupling, the so-called “weak” dipole moment form factor (WDM)  $d_\tau^Z(q^2)$ . These are expected to be unobservably small in the SM. Thus, observation of  $CP$ -violation in production would be unambiguous evidence for physics beyond the SM. The signal for  $CP$ -violation in  $\tau$  production would be the non-zero values of momentum correlations between the  $\tau$  decay products, which we discuss in the subsequent sections [1, 2].

TESLA is a proposed  $e^+e^-$  linear collider with a center-of-mass energy of  $\sqrt{s} = 500$  GeV with the possibility of an extension to 800 GeV [4]. It is a multi-purpose machine that will test various aspects of the standard model (SM) and search for signals of interactions beyond the standard model. A strong longitudinal polarization program at TESLA with considerable polarization of the electron beam, with the possibility of some although not a high degree of polarization of the positron beam is also planned [5]. We assume an integrated luminosity of a few hundred  $\text{fb}^{-1}$ , which would lead to copious production of  $\tau^+\tau^-$  pairs. Longitudinal beam polarization of the electron and positron beams would lead to a substantial enhancement of certain vector correlations, which are non-vanishing in the event that the  $\tau$  lepton has an EDM or a WDM. We

will assume integrated luminosities of 500 and 1000  $\text{fb}^{-1}$  at center-of-mass energies of 500 and 800 GeV, respectively. We expect a magnitude of polarization of 80% for the electron beam and 60% for the positron beam.

Our aim in this work is to study these vector correlations constructed from the momenta of the charged decay products of  $\tau$  leptons. We will confine our attention to two-body decays of the  $\tau$  leptons for which the correlations as well as their variance due to  $CP$ -conserving standard model interactions can be computed analytically. We also study the effects of helicity-flip bremsstrahlung [6] which contributes to these correlations at  $\mathcal{O}(\alpha)$ . This is a standard model background to the signal of interest.

Note that it is also possible to consider tensor correlations among the momenta and these have been investigated for the unpolarized case in [2] for these energies. The vector correlations are substantially enhanced by longitudinal beam polarization, but not the tensor correlations. This may be traced back to the effective polarization of the photon or the  $Z^0$  at the electronic vertex of the corresponding Feynman diagrams. Therefore we consider only vector correlations.

The plan of the paper is the following: in the next section we present estimates for the EDM and WDM in certain popular extensions of the SM which sets the scale for our studies. In Sect. 3, we discuss the correlations in general and reproduce results from the literature for our vector correlations. In Sect. 4, we discuss the numerical results for TESLA energies, luminosities, and polarizations, including the limits achievable. In Sect. 5 we discuss

the implications of our results for the configuration being planned at TESLA and how our results will translate into certain design criteria for the machine and the detector. Discussions and conclusions are presented in Sect. 6.

## 2 Dipole moments in extensions to the standard model

$CP$ -violating dipole moments of leptons can arise in the standard model radiatively. However, since there is no  $CP$ -violation in the lepton sector in SM, it can only be induced by  $CP$ -violation in the quark sector. One has to go at least to three-loop order to generate a non-vanishing contribution to the lepton dipole moments [7,8]. A crude estimate gives

$$|d_\tau(SM)| \lesssim 10^{-34} \text{ e cm.} \quad (1)$$

Extensions of the SM where complex couplings appear can easily generate  $CP$ -violating dipole moments for the  $\tau$  lepton at one-loop order. Provided these couplings are generation or mass dependent, it is possible that reasonably large dipole moments for the  $\tau$  lepton are generated, while continuing to satisfy the constraints coming from strong limits on the electric dipole moments of the electron or the neutron.

Since dipole couplings of fermions are chirality flipping, they would be proportional to a fermionic mass. However, this need not necessarily be the mass of the  $\tau$  lepton. It could be the mass of some other heavy fermion in the theory. As a result, the dipole coupling at energy of  $\sqrt{s}$  need not necessarily be suppressed by a factor of  $m_\tau/\sqrt{s}$ , but could involve a factor  $m_F/\sqrt{s}$ , where  $F$  is a heavy particle, possibly a new particle in the extension of the SM, and this factor need not be small. For example, in the model with third generation scalar leptopquarks which couple tau leptons to top quarks, the mass appearing is the top-quark mass [9,10]. The dipole coupling of  $\tau$  induced at one loop takes the form

$$d_\tau = \frac{eg_l^2}{4\pi s} \cdot m_t \cdot F, \quad (2)$$

where  $g_l$  is the leptoquark coupling constant,  $m_t$  is the top mass, and  $F(s)$  is a function of dimensionless quantities, which is at most of order 1.

It is thus possible to get dipole form factors almost of the order of  $(\alpha/\pi)$  in units of an inverse mass which appears in the loop. If the mass is that of  $W$  or  $Z$ , it is possible to get dipole moments of the order of  $10^{-19}$  e cm. In actual practice, however, the particle appearing in the loop is also constrained to be heavy. As a result, the dipole moments in left-right symmetric models, Higgs exchange model with spontaneous  $CP$ -violation and natural flavor conservation, and supersymmetric models turn out to be of the order of  $10^{-23}$  e cm, or smaller [7].

In the case of most models, information exists in the literature for the values of electric and weak dipole form factors only at  $q^2$  values of 0 and  $m_\tau^2$ , respectively. Models

in which the  $q^2$  dependence of the  $CP$ -violating form factors has been studied are scalar leptoquark models with couplings only to the third generation of quarks and leptons. Of these, the most promising model is the one in which the leptoquark transforms as an  $SU(2)$  doublet. In [9] a value of  $\text{Re}d_\tau^\gamma \lesssim 3 \cdot 10^{-19}$  e cm was found above the  $Z$  resonance, with  $\text{Re}d_\tau^Z$  about 1/4 of this value for a more favorable case. Taking into account restrictions on the doublet leptoquark mass and couplings coming from LEP data values of  $d_\tau^\gamma \lesssim 10^{-19}$  e cm and  $d_\tau^Z \lesssim (\text{few}) \cdot 10^{-20}$  e cm were estimated at  $\sqrt{q^2} = 500$  GeV [10].

Values of  $\tau$  dipole form factors of the order of  $10^{-19}$  e cm are also obtained in models with Majorana neutrinos of mass of a few hundred GeV, and of the order of  $10^{-20}$  e cm in two-Higgs doublet extensions with natural flavor conservation, and in supersymmetric models through a complex  $\tau$ - $\tilde{\tau}$ -neutralino coupling, not far from the  $\tilde{\tau}$  threshold [9].

Care must however be exercised in the use of form factors which correspond to off-shell Green's functions, rather than on-shell amplitudes. These may not always be gauge invariant. Limits on form factors obtained from experiments where the photon or  $Z$  is not on-shell should be understood as approximate.

## 3 The vector correlations

In [1] an extensive analysis of momentum correlations was first presented in the context of the reaction  $e^+e^- \rightarrow Z^0 \rightarrow \tau^+\tau^-$ , and was subsequently generalized to energies far away from the  $Z$  resonance in [2]. Expressions were presented there for the  $\tau$  production matrix  $\chi$  involving the EDM and the WDM, in addition to the main contribution from SM vertices, which is required to compute the production cross section, the momentum correlations of interest, as well as their variances, also taking into account the  $\mathcal{D}$  matrices that account for the decay of the  $\tau$  into (two-body) final states. In [11] it was shown that in the limit of vanishing electron mass, the initial state depends on the electron polarization  $P_e$  and the positron polarization  $P_{\bar{e}}$  only through the  $CP$ -even combinations  $(P_e - P_{\bar{e}})$  and  $(1 - P_e P_{\bar{e}})$ . Therefore one may search for  $CP$ -violation through the non-vanishing expectation values of  $CP$ -odd momentum correlations for arbitrary electron and positron polarizations. In particular, simple ‘‘vector’’ correlations for which the correlations as well as their variances could be computed in closed form were shown to have enhanced sensitivity to  $CP$ -violating EDM and WDM of the  $\tau$  leptons at SLC, and at the energies of a Tau-charm factory. In this work, we shall examine these correlations for their sensitivity to  $\tau$  EDM and WDM at TESLA energies, polarizations and luminosities.

The  $CP$ -odd momentum correlations we consider here are associated with the center-of-mass momenta  $\mathbf{q}_{\bar{B}}$  of  $\bar{B}$  and  $\mathbf{q}_A$  of  $A$ , where the  $\bar{B}$  and  $A$  arise in the decays  $\tau^+ \rightarrow \bar{B}\bar{\nu}_\tau$  and  $\tau^- \rightarrow A\nu_\tau$ , and where  $A, B$  run over  $\pi, \rho, a_1$ , etc. In the case when  $A$  and  $B$  are different, one has to

consider also the decays with  $A$  and  $B$  interchanged, so as to construct correlations which are explicitly  $CP$ -odd.

The correlations we consider are

$$O_1 \equiv \frac{1}{2} [\hat{\mathbf{p}} \cdot (\mathbf{q}_{\bar{B}} \times \mathbf{q}_A) + \hat{\mathbf{p}} \cdot (\mathbf{q}_{\bar{A}} \times \mathbf{q}_B)] \quad (3)$$

and

$$O_2 \equiv \frac{1}{2} [\hat{\mathbf{p}} \cdot (\mathbf{q}_A + \mathbf{q}_{\bar{B}}) + \hat{\mathbf{p}} \cdot (\mathbf{q}_{\bar{A}} + \mathbf{q}_B)], \quad (4)$$

where  $\hat{\mathbf{p}}$  is the unit vector in the positron beam direction.

Note that since  $O_2$  is  $CPT$ -odd it measures  $\text{Im}d_\tau^i$ , whereas  $O_1$  is  $CPT$ -even and measures  $\text{Re}d_\tau^i$ . An additional advantage of these correlations is that the correlations as well as the standard deviation for the operators due to the standard model background are both calculable in closed form for two-body decays of the  $\tau$  leptons.

The calculations include two-body decay modes of the  $\tau$  in general and are applied specifically to the case of  $\tau \rightarrow \pi\nu_\tau$  and  $\tau \rightarrow \rho\nu_\tau$  due to the fact that these modes possess a good resolving power of the  $\tau$  polarization, parameterized in terms of the constant  $\alpha_\pi = 1$  for the  $\pi$  channel (with branching fraction of about 11%) and  $\alpha_\rho = 0.46$  for the  $\rho$  channel (with branching fraction of about 25%) from the momentum of the  $\pi$  or the  $\rho$ .

Analytic expressions for these correlations can be found in [12]. For the sake of convenience of reference and completeness, we give the expressions here. With the definitions  $r_{ij} \equiv (V_e^i A_e^j + V_e^j A_e^i) / (V_e^i V_e^j + A_e^i A_e^j)$  and the effective polarization parameter  $P \equiv (P_e - P_{\bar{e}}) / (1 - P_e P_{\bar{e}})$  (the vector and axial-vector couplings  $A_l^i, V_l^i, l = e$  or  $\tau, i = \gamma$  or  $Z$  are listed in [2]),

$$\begin{aligned} \langle O_1 \rangle = & -\frac{1}{36x\sigma} \sum_{i,j} K_{ij} s^{3/2} m_\tau^2 (1-x^2) \left( \frac{r_{ij} - P}{1 - r_{ij}P} \right) \\ & \times \left[ (A_\tau^i \text{Re } d_\tau^j + A_\tau^j \text{Re } d_\tau^i) \alpha_A \alpha_B (1-p_A)(1-p_B) \right. \\ & - \frac{3}{2} (V_\tau^i \text{Re } d_\tau^j + V_\tau^j \text{Re } d_\tau^i) [\alpha_A (1-p_A)(1+p_B) \\ & \left. + \alpha_B (1-p_B)(1+p_A)] \right], \quad (5) \end{aligned}$$

and

$$\begin{aligned} \langle O_2 \rangle = & \frac{1}{3\sigma} \sum_{i,j} K_{ij} s^{3/2} m_\tau \left( \frac{r_{ij} - P}{1 - r_{ij}P} \right) \\ & \times \frac{1}{4} (A_\tau^i \text{Im } d_\tau^j + A_\tau^j \text{Im } d_\tau^i) (1-x^2) \\ & \times (\alpha_A (1-p_A) + \alpha_B (1-p_B)), \quad (6) \end{aligned}$$

where  $x = 2m_\tau / (\sqrt{s})$ ,  $p_{A,B} = m_{A,B}^2 / m_\tau^2$ , and  $\sigma$  is the cross section of  $e^+e^- \rightarrow \tau^+\tau^-$  given by

$$\sigma = \sum_{i,j} K_{ij} s \left[ V_\tau^i V_\tau^j \left( 1 + \frac{x^2}{2} \right) + A_\tau^i A_\tau^j (1-x^2) \right], \quad (7)$$

and

$$K_{ij} = \frac{(V_e^i V_e^j + A_e^i A_e^j)(1 - r_{ij}P)}{12\pi(s - M_i^2)(s - M_j^2)} \sqrt{1-x^2} [1 - P_e P_{\bar{e}}]. \quad (8)$$

Since the energies involved are far above the  $Z$  resonance, we have neglected the  $Z$  width in the expressions above.

We have analytic expressions for the variance  $S_a^2 \equiv \langle O_a^2 \rangle - \langle O_a \rangle^2 \approx \langle O_a^2 \rangle$  in each case, arising from the  $CP$ -invariant SM part of the interaction:

$$\begin{aligned} \langle O_1^2 \rangle = & \frac{1}{720x^2\sigma} \sum_{i,j} K_{ij} s m_\tau^4 \left( (1-p_A)^2 (1-p_B)^2 \right. \\ & \times [V_\tau^i V_\tau^j (6 + 8x^2 + x^4) + A_\tau^i A_\tau^j (6 - 2x^2 - 4x^4)] \\ & + (1-x^2) \\ & \times [(1+p_A)^2 (1-p_B)^2 + (1+p_B)^2 (1-p_A)^2] \\ & \times [3V_\tau^i V_\tau^j (3 + 2x^2) + 9A_\tau^i A_\tau^j (1-x^2)] \\ & + 4(1-x^2)^2 \alpha_A \alpha_B (1-p_B^2)(1-p_A^2) \\ & \times [V_\tau^i V_\tau^j - A_\tau^i A_\tau^j] \\ & - 6(1-x^2) \left( 1 - \frac{x^2}{6} \right) (1-p_A)(1-p_B) \\ & \times [V_\tau^i A_\tau^j + V_\tau^j A_\tau^i] \\ & \left. \times [\alpha_A (1+p_A)(1-p_B) + \alpha_B (1+p_B)(1-p_A)] \right), \quad (9) \\ \langle O_2^2 \rangle = & \frac{1}{360x^2\sigma} \sum_{i,j} K_{ij} s m_\tau^2 \left[ (3[(1-p_A)^2 + (1-p_B)^2] \right. \\ & \times [V_\tau^i V_\tau^j (4 + 7x^2 + 4x^4) + A_\tau^i A_\tau^j 2(1-x^2)(2 + 3x^2)] \\ & - 2\alpha_A \alpha_B (1-p_A)(1-p_B) \\ & \times [V_\tau^i V_\tau^j (4 + 7x^2 + 4x^4) + A_\tau^i A_\tau^j 4(1-x^2)^2] \\ & + 6 \left( 6(1-x^2)(p_A - p_B)^2 \right. \\ & \times \left[ V_\tau^i V_\tau^j \left( 1 + \frac{x^2}{4} \right) + A_\tau^i A_\tau^j (1-x^2) \right] \\ & - (1-x^2)(4+x^2)(p_A - p_B) \\ & \times [\alpha_A (1-p_A) - \alpha_B (1-p_B)] \\ & \left. \left. \times [V_\tau^i A_\tau^j + V_\tau^j A_\tau^i] \right) \right]. \quad (10) \end{aligned}$$

The expected uncertainty (one standard deviation) on the measurement of  $d_\tau$  can then be calculated from

$$\begin{aligned} \delta \text{Re}(\text{Im})d_\tau^i = & \frac{1}{c_{AB}^{a,i}} \frac{e}{\sqrt{s}} \frac{1}{\sqrt{N_{AB}}} S_a, \quad (11) \\ & a = 1(\text{Re}), 2(\text{Im}), \quad i = \gamma, Z. \end{aligned}$$

The electric charge of the electron is denoted by  $e$ . The  $c_{AB}^{a,i}$  are respective coefficients of  $\text{Re}d_\tau^i$  ( $a = 1$ ) and  $\text{Im}d_\tau^i$  ( $a = 2$ ) occurring in the expressions (5) and (6) for  $\langle O_{1,2} \rangle$ , and are discussed in the next section.  $N_{AB}$  is the number of events in the channel  $A\bar{B}$  and  $\bar{A}B$ , and is given by

$$N_{AB} = N_{\tau^+\tau^-} B(\tau^- \rightarrow A\nu_\tau) B(\tau^+ \rightarrow \bar{B}\bar{\nu}_\tau), \quad (12)$$

where we compute  $N_{\tau^+\tau^-}$  for the design luminosities and from the cross section at the given energy and the polarizations.

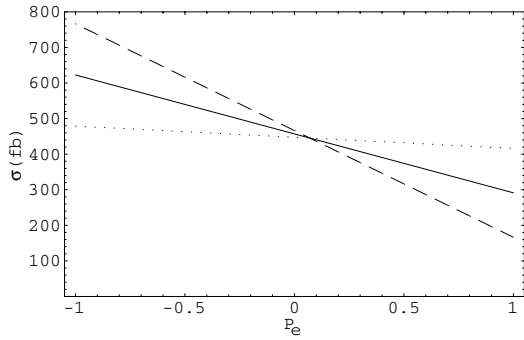


**Fig. 1.** Values of the cross section for  $P_{\bar{e}} = 0, 0.3, 0.6$  (dotted, solid and dashed) as a function of  $P_e$ , with  $\sqrt{s} = 500$  GeV

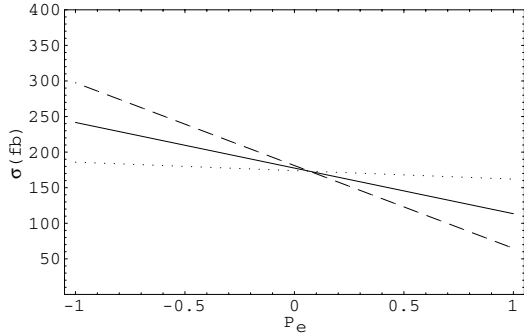


**Fig. 2.** Values of the cross section for  $P_{\bar{e}} = 0, 0.3, 0.6$  (dotted, solid and dashed) as a function of  $P_e$ , with  $\sqrt{s} = 800$  GeV

**Table 1.** Coefficients  $\sigma_1$  and  $\sigma_2$  (in units of fb) in the expression for the cross section in (13) for energies of interest

$\sqrt{s}$ (GeV)	$\sigma_1$ (fb)	$\sigma_2$ (fb)
500	447.70	-31.37
800	174.03	-11.94

### 4 Results for TESLA

Here we present the results for the vector correlations and their standard deviation at TESLA energies, luminosities and polarizations, using the expressions of the previous section.

We begin with the expression for the cross section which is of the form

$$\sigma_1(1 - P_e P_{\bar{e}}) + \sigma_2(P_e - P_{\bar{e}}) \tag{13}$$

The quantity  $\sigma_1$  is simply the cross section in the absence of beam polarization and  $\sigma_2$  measures the polarization dependent part of the cross section, when only one beam is polarized. So when either electron or positron beam has polarization  $+P$  or  $-P$ , respectively, the cross section is  $\sigma_1 + P\sigma_2$ . The values of  $\sigma_1$  and  $\sigma_2$  for the energies of interest are given in Table 1. Since  $\sigma_2$  is negative and much smaller in magnitude compared to  $\sigma_1$ , the cross section for an unpolarized positron beam has a small negative slope with respect to the electron polarization. This can be seen from Fig. 1, where we present profiles of the cross section as a function of  $P_e$  for values of the positron polarization

of  $P_{\bar{e}} = 0, 0.3$  and  $0.6$  for  $\sqrt{s} = 500$  GeV. The situation at  $\sqrt{s} = 800$  GeV is presented in Fig. 2. We will, for the rest of the discussion, consider these to be the reference polarizations for the positron beam. Notice that the cross section is larger when the  $e^+$  and  $e^-$  polarizations are opposite in sign, and that it increases with  $e^+$  polarization. This results in better sensitivities for the corresponding cases.

Analogously, the expressions for the quantities  $c_{AB}^{a,i}$  (defined in the previous section as coefficients occurring in  $\langle O_{1,2} \rangle$ ) and  $\langle O_a^2 \rangle$  may be schematically expressed by

$$c_{AB}^{a,i} = f \frac{C_1^{a,i}(1 - P_e P_{\bar{e}}) + C_2^{a,i}(P_e - P_{\bar{e}})}{\sigma_1(1 - P_e P_{\bar{e}}) + \sigma_2(P_e - P_{\bar{e}})}, \tag{14}$$

$a = 1, 2, \quad i = \gamma, Z,$

and

$$\langle O_a^2 \rangle = f \frac{D_1^a(1 - P_e P_{\bar{e}}) + D_2^a(P_e - P_{\bar{e}})}{\sigma_1(1 - P_e P_{\bar{e}}) + \sigma_2(P_e - P_{\bar{e}})}, \quad a = 1, 2. \tag{15}$$

respectively for the operators  $O_1$  and  $O_2$ , where  $f = 4\pi\alpha^2 (\hbar c)^2/3 = 9.818 \cdot 10^7 \text{ GeV}^2 \text{ fb}$ . We have taken  $\alpha^{-1} = 128.87$ . The quantities  $C_k^{a,i}$  and  $D_k^a$  are listed in Tables 2–5 for the different energies and channels. Note that the overall dimensions for  $c_{AB}^{1,i}$  and  $c_{AB}^{2,i}$ ,  $i = \gamma, Z$  are  $\text{GeV}^2$  and  $\text{GeV}$  respectively and that of  $\langle O_1^2 \rangle$  and  $\langle O_2^2 \rangle$  are  $\text{GeV}^4$  and  $\text{GeV}^2$  respectively, which for brevity will not be mentioned in the rest of the discussion.

In order to get a feeling for the dependence of the quantities of interest on the polarization, we illustrate the  $\pi\pi$  channel. In Fig. 3, we present  $c_{\pi\pi}^{1,\gamma}$  as a function of  $P_e$ . The sign of  $P_e$  is opposite to  $P_{\bar{e}}$  in order to maximize the effects of longitudinal polarization. Also in Fig. 3, we have an analogous illustration of  $c_{\pi\pi}^{1,Z}$ . It differs substantially from the  $\gamma$  case, due to the different sizes and signs of the coefficients  $C_k^{1,i}$  that enter the final expressions for  $c_{\pi\pi}^{1,i}$ . In Fig. 4, we present profiles of the quantity  $S_1$  for the  $\pi\pi$  channel, where  $S_1$  is the sensitivity of the channel as defined in (11). In Fig. 5 we illustrate the behavior of  $c_{\pi\pi}^{2,\gamma}$  and  $c_{\pi\pi}^{2,Z}$ , which correspond to coefficients of  $\text{Im}d_\tau^i$ . For maximum electron polarization  $P_e = \pm 1$  all quantities become independent of  $P_{\bar{e}}$ , since the effective polarization parameter no longer depends on  $P_{\bar{e}}$  ( $P = \pm 1$ ). We do not illustrate the behavior of  $S_2$  since this quantity is practically constant with a value of 52.40 in the entire range of the positron polarization. We have not plotted the corresponding curves for the channels involving the  $\rho$  and these may be simply generated from the entries given in the tables.

We now discuss the limits achievable at TESLA with the design luminosities and polarizations (we give one standard deviation uncertainties). With a fixed value of electron and positron polarizations, one can only obtain limits on linear combinations of the EDM and WDM. Such limits would be defined by straight lines given by the equation

$$\frac{\delta \text{Red}_\tau^\gamma}{a} + \frac{\delta \text{Red}_\tau^Z}{b} = \pm 1 \tag{16}$$

for the limits arising from  $O_1$  and by

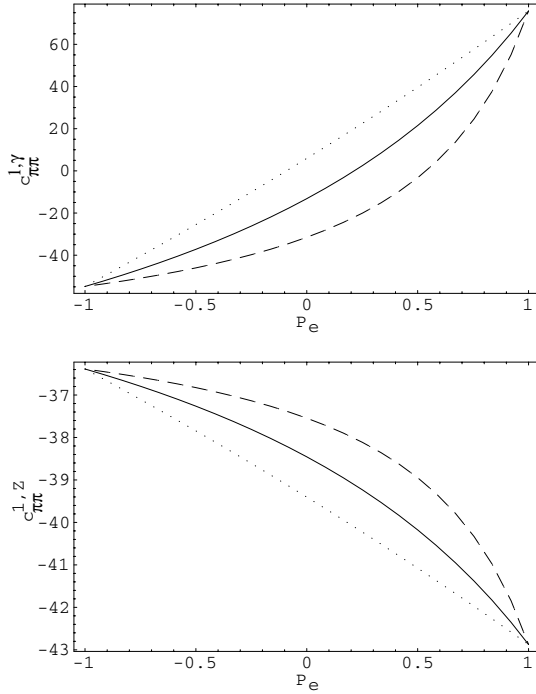


**Fig. 3.** Values of  $c_{\pi\pi}^{1,\gamma}$  (upper plot) and  $c_{\pi\pi}^{1,Z}$  for  $P_{\bar{e}} = 0, 0.3, 0.6$  (dotted, solid and dashed) as a function of  $P_e$ , with  $\sqrt{s} = 500$  GeV

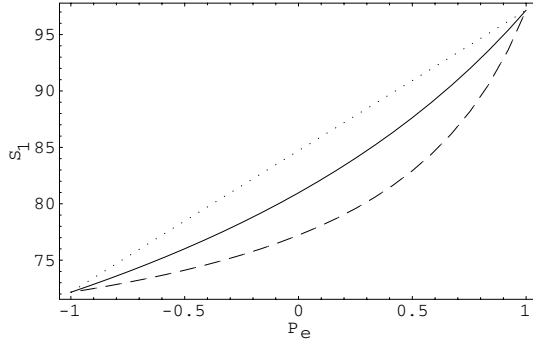


**Fig. 4.** Values of  $S_1$  for  $P_{\bar{e}} = 0, 0.3, 0.6$  (dotted, solid and dashed) as a function of  $P_e$ , with  $\sqrt{s} = 500$  GeV

$$\frac{\delta \text{Im}d_{\tau}^{\gamma}}{c} + \frac{\delta \text{Im}d_{\tau}^Z}{d} = \pm 1 \quad (17)$$

for the limits arising from  $O_2$  where the numbers  $a$ ,  $b$ ,  $c$ , and  $d$  can be explicitly computed for given polarizations and luminosities. The value of  $a$  ( $c$ ) is the sensitivity to the real (imaginary) part of the EDM when the real (imaginary) part of the WDM is set to zero and  $b$  ( $d$ ) is the sensitivity to the WDM when the EDM is set to zero.

The quantities  $a$ ,  $b$ ,  $c$ , and  $d$  are plotted in Figs. 6–9 as functions of  $P_e$  in the vicinity of  $P_e = -0.8$ , for the reference values of  $P_{\bar{e}}$ . In all cases, the variation with  $P_e$  and  $P_{\bar{e}}$  is slow in the range we have chosen, since we are already close to the maximum effective polarization. Many models predict a significantly larger EDM than WDM. In this case the limits achievable are precisely  $a$  and  $c$  on the real and imaginary parts of the EDM. If this is not the

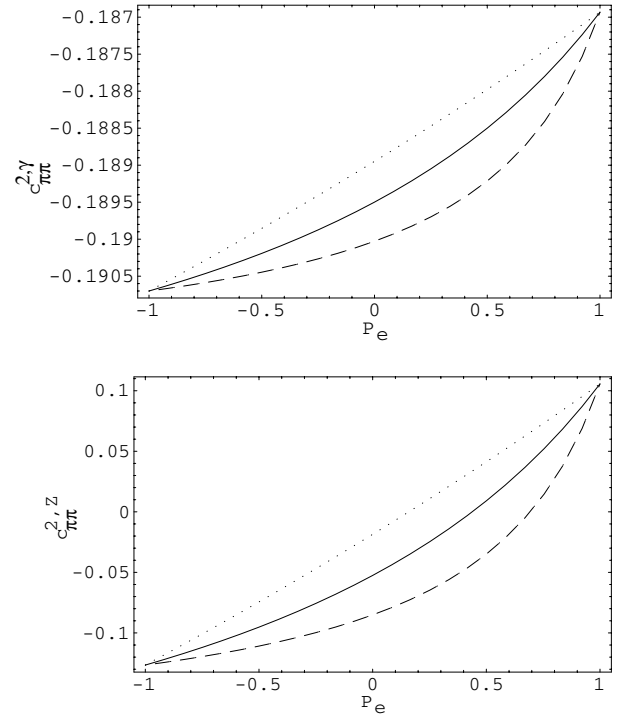


**Fig. 5.** Values of  $c_{\pi\pi}^{2,\gamma}$  (upper plot) and  $c_{\pi\pi}^{2,Z}$  for  $P_{\bar{e}} = 0, 0.3, 0.6$  (dotted, solid and dashed) as a function of  $P_e$ , with  $\sqrt{s} = 500$  GeV

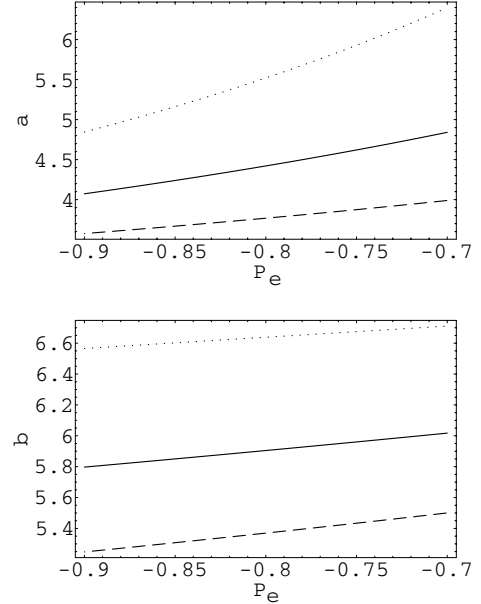


**Fig. 6.** Values of  $a$  and  $b$  (in units of  $10^{-19}$  e cm) for  $P_{\bar{e}} = 0, 0.3, 0.6$  (dotted, solid and dashed) as a function of  $P_e$  in the vicinity of the expected value of  $-0.8$  for  $\int dt \cdot \mathcal{L} = 500 \text{ fb}^{-1}$  and  $\sqrt{s} = 500$  GeV

case, the EDM and WDM can be disentangled by switching the relative signs of  $P_e$  and  $P_{\bar{e}}$ . For the observable  $O_1$ , two straight lines are achieved in the plane of  $\text{Re}d_{\tau}^{\gamma}$  versus  $\text{Re}d_{\tau}^Z$  given by (16). With the polarization reversed another two lines are obtained forming a parallelogram. Its corners are given by  $(\pm\mathcal{A}, \pm\mathcal{B})$ . The experiment can

**Table 2.** List of coefficients for the operator  $O_1$  for  $\sqrt{s} = 500$  GeV

$AB$	$C_1^{1,\gamma}$	$C_2^{1,\gamma}$	$C_1^{1,Z}$	$C_2^{1,Z}$	$D_1^1$	$D_2^1$
$\pi\pi$	$2.70 \cdot 10^{-5}$	$2.94 \cdot 10^{-4}$	$-1.79 \cdot 10^{-4}$	$-2.12 \cdot 10^{-6}$	$3.27 \cdot 10^{-2}$	$7.31 \cdot 10^{-3}$
$\pi\rho$	$6.67 \cdot 10^{-6}$	$2.30 \cdot 10^{-4}$	$-1.41 \cdot 10^{-4}$	$7.22 \cdot 10^{-6}$	$2.92 \cdot 10^{-2}$	$3.28 \cdot 10^{-3}$
$\rho\rho$	$1.20 \cdot 10^{-6}$	$1.32 \cdot 10^{-4}$	$-8.08 \cdot 10^{-5}$	$5.73 \cdot 10^{-6}$	$2.47 \cdot 10^{-2}$	$1.10 \cdot 10^{-3}$

**Table 3.** List of coefficients for the operator  $O_2$  for  $\sqrt{s} = 500$  GeV

$AB$	$C_1^{2,\gamma}$	$C_2^{2,\gamma}$	$C_1^{2,Z}$	$C_2^{2,Z}$	$D_1^2$	$D_2^2$
$\pi\pi$	$-8.61 \cdot 10^{-7}$	$6.89 \cdot 10^{-8}$	$-8.46 \cdot 10^{-8}$	$5.33 \cdot 10^{-7}$	$1.25 \cdot 10^{-2}$	$-8.77 \cdot 10^{-4}$
$\pi\rho$	$-5.92 \cdot 10^{-7}$	$4.74 \cdot 10^{-8}$	$-5.83 \cdot 10^{-8}$	$3.66 \cdot 10^{-7}$	$1.44 \cdot 10^{-2}$	$-2.38 \cdot 10^{-3}$
$\rho\rho$	$-3.24 \cdot 10^{-7}$	$2.59 \cdot 10^{-8}$	$-3.18 \cdot 10^{-8}$	$2.10 \cdot 10^{-7}$	$1.17 \cdot 10^{-2}$	$-8.17 \cdot 10^{-4}$

**Table 4.** List of coefficients for the operator  $O_1$  for  $\sqrt{s} = 800$  GeV

$AB$	$C_1^{1,\gamma}$	$C_2^{1,\gamma}$	$C_1^{1,Z}$	$C_2^{1,Z}$	$D_1^1$	$D_2^1$
$\pi\pi$	$1.65 \cdot 10^{-5}$	$1.84 \cdot 10^{-4}$	$-1.10 \cdot 10^{-4}$	$-1.09 \cdot 10^{-6}$	$3.26 \cdot 10^{-2}$	$7.17 \cdot 10^{-3}$
$\pi\rho$	$4.08 \cdot 10^{-6}$	$1.44 \cdot 10^{-4}$	$-8.64 \cdot 10^{-5}$	$4.47 \cdot 10^{-6}$	$2.92 \cdot 10^{-2}$	$3.22 \cdot 10^{-3}$
$\rho\rho$	$7.35 \cdot 10^{-7}$	$8.22 \cdot 10^{-5}$	$-4.95 \cdot 10^{-4}$	$3.52 \cdot 10^{-6}$	$2.46 \cdot 10^{-2}$	$1.10 \cdot 10^{-3}$

**Table 5.** List of coefficients for the operator  $O_2$  for  $\sqrt{s} = 800$  GeV

$AB$	$C_1^{2,\gamma}$	$C_2^{2,\gamma}$	$C_1^{2,Z}$	$C_2^{2,Z}$	$D_1^2$	$D_2^2$
$\pi\pi$	$-3.29 \cdot 10^{-7}$	$2.63 \cdot 10^{-8}$	$-3.17 \cdot 10^{-8}$	$2.00 \cdot 10^{-7}$	$1.25 \cdot 10^{-2}$	$-8.54 \cdot 10^{-4}$
$\pi\rho$	$-2.26 \cdot 10^{-7}$	$1.81 \cdot 10^{-8}$	$-2.18 \cdot 10^{-8}$	$1.37 \cdot 10^{-7}$	$1.43 \cdot 10^{-2}$	$-2.32 \cdot 10^{-3}$
$\rho\rho$	$-1.24 \cdot 10^{-7}$	$9.92 \cdot 10^{-9}$	$-1.19 \cdot 10^{-8}$	$7.51 \cdot 10^{-8}$	$1.16 \cdot 10^{-2}$	$-7.96 \cdot 10^{-4}$

**Table 6.** Sensitivities achievable independently for the EDM and WDM form factors when relative sign of electron and positron polarizations is reversed

$\sqrt{s}$ (GeV)	$\mathcal{A}$	$\mathcal{B}$	$\mathcal{C}$	$\mathcal{D}$
500	$3.73 \cdot 10^{-20}$	$-5.90 \cdot 10^{-19}$	$-9.31 \cdot 10^{-17}$	$3.15 \cdot 10^{-18}$
	$-3.84 \cdot 10^{-19}$	$1.03 \cdot 10^{-20}$	$1.05 \cdot 10^{-17}$	$-1.60 \cdot 10^{-16}$
800	$2.63 \cdot 10^{-20}$	$-4.25 \cdot 10^{-19}$	$-1.07 \cdot 10^{-16}$	$3.90 \cdot 10^{-18}$
	$-2.71 \cdot 10^{-19}$	$7.39 \cdot 10^{-21}$	$1.22 \cdot 10^{-17}$	$-1.88 \cdot 10^{-16}$

only limit the values of  $\text{Re}d_\tau^\gamma$  and  $\text{Re}d_\tau^Z$  to fall inside this parallelogram. Taking  $\mathcal{A}$  and  $\mathcal{B}$  to be positive,  $(-\mathcal{A}, -\mathcal{B})$  and  $(\mathcal{A}, \mathcal{B})$  correspond to the most extreme values of the EDM and WDM allowed by experiment. They represent the independent limits on the real part of the EDM and WDM form factors. Similar arguments apply to the imaginary parts. The limits achievable for equal luminosities for both settings are given in Table 6.

We also present in Table 7 numbers computed for the contribution from the helicity-flip bremsstrahlung to the operator  $O_2$ . We schematically express it as

$$\langle O_2 \rangle_{\text{SM}} = \frac{-A'(P_e + P_{\bar{e}})}{\sigma_1(1 - P_e P_{\bar{e}}) + \sigma_2(P_e - P_{\bar{e}})} \quad (18)$$

where the quantity  $\langle O_2 \rangle_{\text{SM}}$  has the overall dimension of GeV, and the corresponding coefficient  $A'$  is tabulated in

**Table 7.** Coefficient  $A'$  of helicity-flip bremsstrahlung to  $\langle O_2 \rangle_{\text{SM}}$ 

$AB$	$\sqrt{s} = 500$ GeV	$\sqrt{s} = 800$ GeV
$\pi\pi$	338	243
$\pi\rho$	343	242
$\rho\rho$	349	241

Table 7. The cross sections  $\sigma_i$  are given in Table 1. Even with extreme values of  $P_e$  and  $P_{\bar{e}}$ , we get a number of order 1, to be contrasted with  $S_2 \simeq 50$  for the  $\pi\pi$  channel. For the expected statistics the effect can be corrected using the expressions given above.

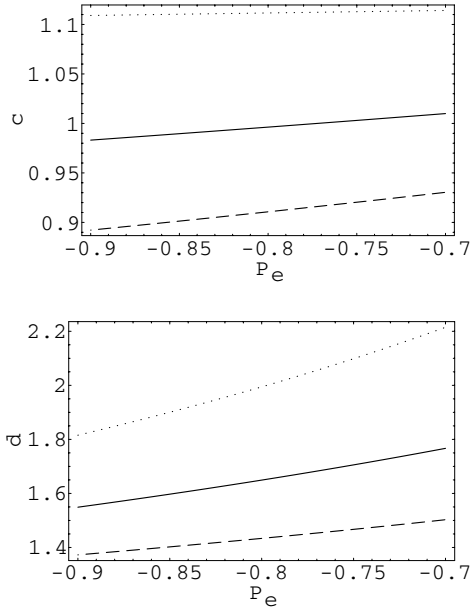


**Fig. 7.** Values of  $c$  and  $d$  (in units of  $10^{-16} e \text{ cm}$ ) for  $P_{\bar{\tau}} = 0, 0.3, 0.6$  (dotted, solid and dashed) as a function of  $P_e$  in the vicinity of the expected value of  $-0.8$  for  $\int dt \cdot \mathcal{L} = 500 \text{ fb}^{-1}$  and  $\sqrt{s} = 500 \text{ GeV}$

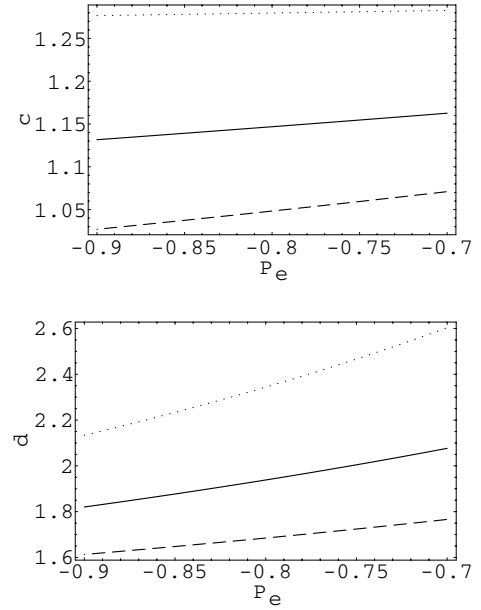


**Fig. 9.** Values of  $c$  and  $d$  (in units of  $10^{-16} e \text{ cm}$ ) for  $P_{\bar{\tau}} = 0, 0.3, 0.6$  (dotted, solid and dashed) as a function of  $P_e$  in the vicinity of the expected value of  $-0.8$  for  $\int dt \cdot \mathcal{L} = 1000 \text{ fb}^{-1}$  and  $\sqrt{s} = 800 \text{ GeV}$

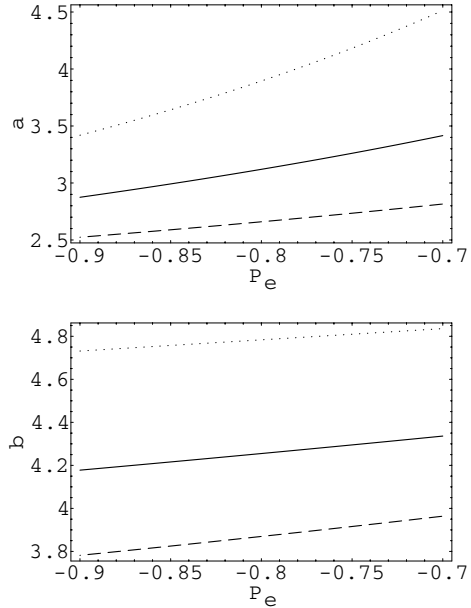


**Fig. 8.** Values of  $a$  and  $b$  (in units of  $10^{-19} e \text{ cm}$ ) for  $P_{\bar{\tau}} = 0, 0.3, 0.6$  (dotted, solid and dashed) as a function of  $P_e$  in the vicinity of the expected value of  $-0.8$  for  $\int dt \cdot \mathcal{L} = 1000 \text{ fb}^{-1}$  and  $\sqrt{s} = 800 \text{ GeV}$

TESLA can also be operated at the  $Z$  pole. It is expected that sufficient integrated luminosity will be available to generate as many as  $10^9$   $Z$  bosons. In this mode of running at TESLA, which has been named GIGAZ, a simple scaling of the limits obtained in [11] can be performed. Here with the effective polarization parameter  $P \simeq 0.95$  we would obtain 1 s.d. limits of  $3 \times 10^{-19} e \text{ cm}$  on the real

part, and  $10^{-18} e \text{ cm}$  on the imaginary part of the weak dipole moment.

## 5 Experimental aspects

Up to this point we have done analytic calculations of vector correlations for two decay channels of the  $\tau$  lepton. This gives us a realistic estimate of the limits that can be achieved on the EDM and WDM with these decays with a perfect detector. Here we want to discuss possibilities of improving the sensitivity further and we try to estimate by how much the result will be weakened due to detector effects in a real experiment. We will try to extrapolate the size of the detector effects from the experience from the LEP experiments and SLD [13].

(1) In the calculations we have taken into account the decays into  $\pi$  and  $\rho$ . These are the two most important channels. Together they make up 13% of the total branching ratio of  $\tau$  pairs. More channels can be added. The decay modes  $\tau^- \rightarrow \pi^- \pi^+ \pi^- \nu_\tau$  and  $\tau^- \rightarrow \pi^- \pi^0 \pi^0 \nu_\tau$  and the two leptonic decays  $\tau^- \rightarrow e^- \bar{\nu}_e \nu_\tau$  and  $\tau^- \rightarrow \mu^- \bar{\nu}_\mu \nu_\tau$  have been used at LEP/SLC. This increases the potential fraction of the sample used in the analysis to 82%. However, these additional channels have a lower sensitivity to  $CP$ -violation. Taking this into account the theoretically achievable sensitivity increased by a factor of 2.8 for LEP/SLC. There will probably be a similar factor at TESLA.

(2) The real detector will have a finite energy and momentum resolution for the decay products of the  $\tau$  leptons. This affects the calculation of the observables and reduces the sensitivity. The reduction of sensitivity at LEP/SLC

was less than 10% for events without  $\pi^0$  in the final state and in the order of 10% for events with  $\pi^0$  mesons. Despite the higher energies, the relative momentum resolution of the TESLA detector for charged particles should be slightly better than that at LEP/SLC. The energy resolution of the  $\pi^0$ s (causing the main loss of sensitivity at LEP/SLC) should be substantially better at TESLA. We assume that the loss of sensitivity due to finite energy and momentum resolution will not be larger than 10%.

(3) In a real experiment the event samples selected will contain background from misidentified  $\tau$  decays and also from non- $\tau$  pair events. The background dilutes the signal and reduces the sensitivity. This reduction of sensitivity was between 1 and 10 percent at LEP/SLC for the different decay channels. At higher center-of-mass energies at TESLA the higher Lorentz boost of the  $\tau$  leptons makes the identification of their decay channels more difficult. But then we also expect the TESLA detector to have a better performance. Especially the high granularity of the proposed silicon-tungsten electromagnetic calorimeter will simplify  $\tau$  analysis. Overall we do not expect to lose more than 10% in sensitivity due to background.

(4) The real detector will not have 100% efficiency in the identification of the signal. At LEP/SLC typical values for the overall efficiencies ranged between 50 and 90% for the various decay modes of the  $\tau$  pairs. The TESLA detector should perform at least as good as the LEP/SLC detectors.

Without a detailed study based on a full analysis of events with full detector simulation it is impossible to tell by how much the limit achievable in the real experiment will differ from our analytic estimate. From the argument above we conclude that the achievable limit will not be worse than our analytic estimate. It will probably be better by a factor of a few.

In our estimates we have assumed that it is possible to tune both beam energies exactly to  $\sqrt{s}/2$ . This is not necessarily the case. As an estimate of systematic uncertainties we study the impact of a mistune of the positron beam energy by  $\Delta E_+$ . In such a situation even the standard model interactions will induce an expectation value for the operators  $\langle O_1 \rangle$  and  $\langle O_2 \rangle$ , since the center-of-mass frame no longer corresponds to the laboratory frame. There would be no effect on the operator  $O_1$  since it involves only the components of the three-momentum of the  $\tau$  decay products transverse to the beam direction. For the operator  $O_2$  there would be a contribution due to the relative motion of the center-of-mass frame, a situation analogous to that considered in the context of the helicity-flip bremsstrahlung [6] where the photon carries away a fraction of the beam momentum represented by  $1 - \xi$  ( $= \Delta E_+/E_+$ ). Applying the formalism of [6] leads to the following result:

$$\langle O_2 \rangle = \frac{\Xi(s')}{\sigma(s')},$$

where

$$\begin{aligned} \Xi(s) = & -\frac{1-\xi}{2\sqrt{\xi}} \sum_{i,j} \frac{1}{x} K_{ij} s \left[ (E_A^* + E_B^*) \right. \\ & \times \left( V_\tau^i V_\tau^j \left( 1 + \frac{x^2}{2} \right) + A_\tau^i A_\tau^j (1 - x^2) \right) \\ & \left. + \frac{1}{3} (\alpha_A q_A^* + \alpha_B q_B^*) (A_\tau^i V_\tau^j + A_\tau^j V_\tau^i) (1 - x^2) \right], \end{aligned}$$

and  $s'$  is the square of the center-of-mass energy when  $E_- = \sqrt{s}/2$  and  $E_+ = \sqrt{s}/2 - \Delta E_+$ , and  $E_{A(B)}^*$  and  $q_{A(B)}^*$  denote the energy and momenta of the decay products evaluated in the  $\tau$  rest frame. Carrying out the computations for  $\Delta E_+ = 1$  GeV for  $\sqrt{s} = 500$  GeV, we find  $|\langle O_2 \rangle|$  to be in the range 0.61 to 0.41 GeV when  $P_e$  varies over its allowed range for the  $\pi\pi$  channel. This shows that the contribution is similar to that from the helicity-flip bremsstrahlung. We conclude that it is necessary to control the beam energies to a few hundred MeV.

## 6 Discussion and conclusions

In the present work, we have considered vector correlations among the momenta of charged decay products of the  $\tau^\pm$  in two-body decays into final states with  $\pi$  and  $\rho$ . By considering  $CP$ -odd operators which are  $T$ -odd ( $O_1$ ) and  $T$ -even ( $O_2$ ), it is possible to probe the real and imaginary parts of  $CP$ -violating dipole form factors of the  $\tau$  lepton. We expect the precision as in Table 8 (one standard deviation) with the expected beam polarizations of  $-80\%$  for the electron beam and  $60\%$  for the positron beam (in units of  $e$  cm).

In these determinations the limits on the electric dipole moment are obtained assuming the weak dipole moment is zero and vice versa. It is possible to disentangle the individual limits by switching the beam polarizations (see Table 6).

A priori it cannot be said by how much better tensor correlations of the type considered in [2] will fare when polarization is included and conclusions cannot be drawn unless they are fully studied. However, it must be noted that the sensitivities we have reported here are significantly superior to those obtainable from the tensor correlations with no beam polarization.

**Table 8.** Precision (one standard deviation) with the expected beam polarizations of  $-80\%$  for the electron beam and  $60\%$  for the positron beam (in units of  $e$  cm)

$\sqrt{s}$	$\int dt \mathcal{L}$	$Red_\tau^I$	$Imd_\tau^I$
500 GeV	500 fb $^{-1}$	$3.8 \cdot 10^{-19}$	$0.9 \cdot 10^{-16}$
800 GeV	1000 fb $^{-1}$	$2.7 \cdot 10^{-19}$	$1.1 \cdot 10^{-16}$
		$Red_\tau^Z$	$Imd_\tau^Z$
500 GeV	500 fb $^{-1}$	$5.4 \cdot 10^{-19}$	$1.4 \cdot 10^{-16}$
800 GeV	1000 fb $^{-1}$	$3.9 \cdot 10^{-19}$	$1.7 \cdot 10^{-16}$



The vector correlations are significantly enhanced due to longitudinal polarization of the beams. The precision achievable without polarization would be at least an order of magnitude reduced. Since the effective polarization parameter is already close to unity with the designed electron polarization alone, the gain from positron polarization even at 60% improves the sensitivity by a factor of 2 at most. The measurements are not very sensitive to the precise value of the polarizations. A control on the polarization at the level of a few percent is sufficient.

Furthermore we want to point out that at LEP/SLC a large gain in sensitivity was achieved in moving from the initial tensor observables [14] to optimal observables [15]. This remains to be studied for TESLA energies.

*Acknowledgements.* It is our pleasure to thank Prof. O. Nachtmann for valuable discussions. B.A. thanks the Department of Science and Technology, Government of India, for its support during the course of this work under the project entitled "Some aspects of Low-energy Hadronic Physics".

## References

1. W. Bernreuther, G.W. Botz, O. Nachtmann, P. Overmann, *Z. Phys. C* **52**, 567 (1991)
2. W. Bernreuther, O. Nachtmann, P. Overmann, *Phys. Rev. D* **48**, 78 (1993)
3. Y.S. Tsai, *Phys. Rev. D* **4**, 2821 (1971) [Erratum-ibid. **13**, 771 (1976)]
4. TESLA Technical Design Report Part I-VI, DESY 2001-011
5. G. Moortgat-Pick, H.M. Steiner, *Eur. Phys. J. direct C* **6**, 1 (2001) [hep-ph/0106155]; S.D. Rindani, to appear in Proceedings of the 4th ACFA Workshop on Physics/Detector at the Linear Collider, Beijing, 2001 [hep-ph/0202045]; S.D. Rindani, Proceedings of the Theory Workshop on Physics at Linear Colliders, Tsukuba, 2001, [hep-ph/0105318]
6. B. Ananthanarayan, S.D. Rindani, *Phys. Rev. D* **52**, 2684 (1995)
7. W. Bernreuther, M. Suzuki, *Rev. Mod. Phys.* **63**, 313 (1991) [Erratum-ibid. **64**, 633 (1991)]
8. F. Hoogeveen, *Nucl. Phys. B* **341**, 322 (1990)
9. W. Bernreuther, A. Brandenburg, P. Overmann, *Phys. Lett. B* **391**, 413 (1997)
10. P. Poulou, S.D. Rindani, *Pramana* **51**, 387 (1998)
11. B. Ananthanarayan, S.D. Rindani, *Phys. Rev. Lett.* **73**, 1215 (1994); B. Ananthanarayan, S.D. Rindani, *Phys. Rev. D* **50**, 4447 (1994)
12. B. Ananthanarayan, S.D. Rindani, *Phys. Rev. D* **51**, 5996 (1995)
13. ALEPH, D. Buskulic et al., *Phys. Lett. B* **346**, 371 (1995); L3, M. Acciarri et al., *Phys. Lett. B* **426**, 207 (1998); OPAL, K. Ackerstaff et al., *Z. Phys. C* **74**, 403 (1997); SLD, K. Abe et al., SLAC-PUB-8163
14. W. Bernreuther, U. Low, J.P. Ma, O. Nachtmann, *Z. Phys. C* **43**, 117 (1989); W. Bernreuther, O. Nachtmann, *Phys. Rev. Lett.* **63**, 2787 (1989) [Erratum-ibid. **64**, 1072 (1989)]; W. Bernreuther, O. Nachtmann, *Phys. Lett. B* **268**, 424 (1991); W. Bernreuther, G.W. Botz, O. Nachtmann, P. Overmann, *Z. Phys. C* **52**, 567 (1991)
15. P. Overmann, A New method to measure the tau polarization at the Z peak, University of Dortmund, DO-TH-93-24; D. Atwood, A. Soni, *Phys. Rev. D* **45**, 2405 (1992); M. Diehl, O. Nachtmann, *Z. Phys. C* **62**, 397 (1994)